Investigation of Ti-Pt-V high temperature shape memory alloys towards aerospace applications: a cluster expansion screening

Mordecai Mashamaite[1*], *Phuti* Ngoepe[1], and *Hasani* Chauke[1]

[1]Materials Modelling Centre, University of Limpopo, South Africa

Abstract. TiPt has a higher martensitic transformation above 1200 K, which makes it a good candidate for HTMSAs. However, TiPt exhibits C′ = -32GPa. A new class of Ti-Pt-V systems was predicted using cluster expansion. It was found that the density of the system decreases with the addition of V and the heats of formation was found to be -0.352 eV/atom, suggesting thermodynamical stability. The mechanical behaviour of Ti_2VPt alloy revealed that it is mechanically stable. The phonon dispersion curves confirmed vibrational stability due to the absence of soft modes. This work suggests that the addition of V stabilises and improves the mechanical characteristics of the Ti-Pt alloys.

1 Introduction

The deployment of shape memory alloys (SMAs) with high transformation temperatures has grown significantly in recent years, i.e. alloys that can function at temperatures higher than 400 K [1]. These alloys have potential across various fields including aerospace [2]. A wide range of foundational work has been done on NiTi alloys owing to their excellent behaviour at ambient temperatures [3]. Building on the foundation, NiTi-M (M = Hf, Zr, Pd and Pt) shape memory alloys have been explored for temperatures beyond 400 K. However, these alloys are restricted to martensitic temperatures at about 750 K [4]. Raising the martensitic transformation temperature (MT) is essential for the expansion of high temperature shape memory alloys (HTSMAs). Moreover, improving SMAs strength is also required since plasticity easily occurs at elevated temperatures, leading to an incomplete recovery to deformed shape [5]. Binary alloys such as Ti-Au, Ti-Pd and Ti-Pt have rather high transformation temperatures above 700 K than those of NiTi based alloys [6, 7, 8]. It was found that, the Ti–50Pt displays thermo-elastic MT. Therefore, the TiPt alloy cannot be utilized for high temperature applications due to an ineffective shape memory effect and relatively lower strength in the cubic phase [9]. Theoretically, the equi-atomic B2 TiPt at 50:50 exhibits C' = -32 GPa, which renders the alloy mechanically unstable [10].

Furthermore, Ti-Pt ternary alloying has been investigated to enhance the mechanical characteristics and functionality [11, 12]. According to recent research, it was found that the ternary alloying of V on TiPt has been used to significantly improve the operational and

* Corresponding author: mordecai.mashamaite@ul.ac.za

mechanical properties as well as the MT of the alloys [13]. In this study, we employ cluster expansion and density functional theory to explore new Ti-Pt-V alloys and to examine the structural aspects, thermodynamic and mechanical properties of Ti-Pt-V alloys.

2 Methodology

2.1 Cluster expansion

The UNCLE module was used to carry out the cluster expansion (CE) calculations [14]. The code can anticipate the ground states of three (3) element systems and use a generic algorithm (GA) to accomplish a full cluster expansion fit. This technique was utilized to investigate the thermodynamic and ground state structures of Ti-Pt-V alloys. The fitness of every iteration was examined by mean of the cross-validation score (CVS), this measures the accuracy of prediction of the iterations for the new material/systems. Cross-validation score attempts to minimize the fitting error, as opposed to the conventional mean square error criterion. If the CVS is less than 5 meV/pos, the cluster expansion can be regarded as accurate. The cluster has a total of 8 iterations. The clusters were considered accurate since the CVS score was < 5 meV/pos. which suggests the fitting quality of the cluster expansion.

2.2 Optimization

Within the UNCLE flowchart [14], the total energy simulations of Ti-Pt-V alloys were carried out using Vienna Ab-initio Simulation Package (VASP) [15]. The generalized gradient approximation (GGA) function of Perdew-Burke-Ernzerhof (PBE) [16] was provided to demonstrate the exchange correlation energy. The energy cut-off of 500 eV was employed for the plane-wave expansion of wave functions. The k-points used were sufficient to converge the system [17]. Complete geometry optimization was carried out on the ground-state systems between TiV ↔ TiPt.

3 Results and discussion

Figure 1 illustrates the ground state plot for Ti-Pt-V on the Pt site. From TiV to TiPt alloy, the x denotes composition between the binary alloys. The CE produced a total of 45 new structures. Nine (9) stable structures were found on the ground-state line. It was observed that the initial iteration produced five (5) new structures from the cluster fitting. However, the last iterations produced nine (9) new structures for Ti-Pt-V. Therefore, the final CE includes a total of 45 new structures from the training set, with a CVS score of 0.110 meV/pos.

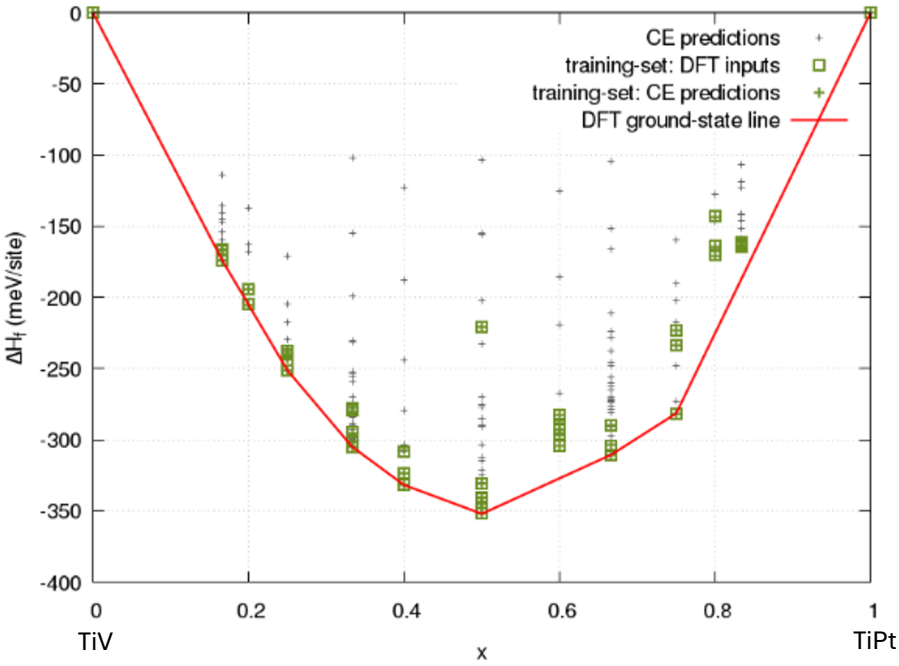

Fig. 1. The ground-state plot of Ti-Pt-V alloys.

In Figure 2(a), the discrepancies for each structure are on the ground-state (red line) of the plot. It is observed that the cluster expansion had a good fit since all the energies lie on the gradient line. In Figure 2(b), it can be noted that the energy differences are in the range 0.002 to -0.002. In addition, it is observed that a larger number (E_{CE} - E_{DFT}) lies closer to 0 for the entire composition range ($0 < x < 1$), which suggests a good cluster fitting.

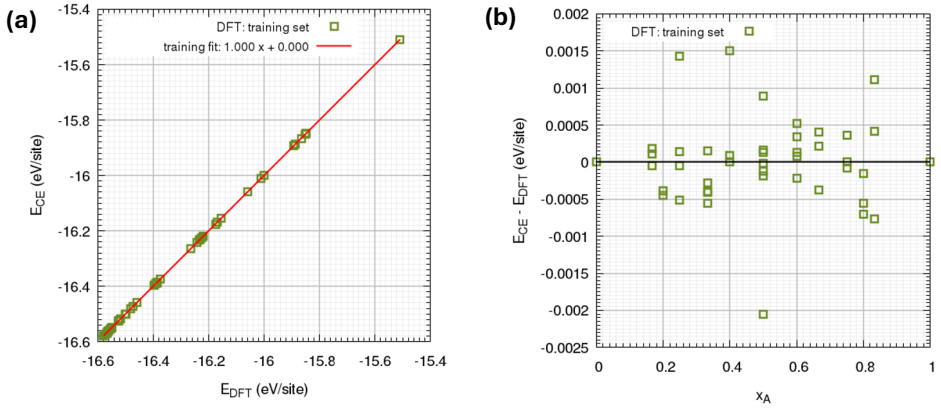

Fig. 2. The fitting errors of the total energy of the (a) E_{CE} - E_{DFT} vs composition and (b) E_{CE} against E_{DFT}.

Ti_2VPt alloy is the most stable structure identified from the binary ground state plot (see Figure. 1), suggesting a thermodynamically stable system since the heats of formation (ΔH_f) [18] were found negative (-0.352 eV/atom). This is since the atomic radius of V (135pm) is equivalent to Pt (135pm), melting point of V (2183 K) is greater than the melting point of Pt

(2041 K). The density of V (6.1 g/cm^3) is lower than that of Pt (21.5 g/cm^3) [11, 12]. This suggests that substitution of the composition of Pt with V is expected to decrease the density of TiPt alloy. The selected alloying element V prefers substitution on the Pt sub-lattice, as suggested by Bozzolo et al. [19].

The elastic constants (C_{ij}) and elastic moduli are fundamental to describing a material's performance under different types of stress. For the Ti_2VPt system, there are C_{11}, C_{12}, C_{13}, C_{33}, C_{44} and C_{66} elastic constants that must satisfy the elastic stability criterion of a tetragonal system in order to be rendered as mechanically stable. The corresponding criteria required for a mechanical stability system are as follows [20]:

$$C_{44} > 0;\ C_{66} > 0;\ C_{11} > |C_{12}| \text{ and } 2C_{13}^2 < C_{33}(C_{11} + C_{12}) \quad (1)$$

The elastic moduli were calculated using the Voigt, Ruess and Hill method [21]. The corresponding elastic moduli derived from these elastic constants are:

$$B_H = \frac{B_V + B_R}{2}, \text{ where } B_{Hill} \text{ is the bulk modulus} \quad (2)$$

$$G_H = \left(\frac{G_V + G_R}{2}\right), G_{Hill} \text{ is the shear modulus} \quad (3)$$

$$E = C_{33} - 2\nu C_{13}, \text{ E is the young's modulus} \quad (4)$$

$$A_1 = \frac{2C_{66}}{C_{11} - C_{12}} \quad (5)$$

$$A_2 = \frac{4C_{44}}{C_{11} + C_{33} - 2C_{13}}, \text{ Where } A_1 \text{ and } A_2 \text{ are elastic anisotropy} \quad (6)$$

The calculated elastic constants in Figure 3 (a) for Ti_2VPt alloys satisfy the stability criterion, suggesting mechanical stability, thus all elastic constants (C_{ij}) are positive. It should be noted that C_{11} is higher (230 GPa), indicating enhanced stiffness in Ti_2VPt alloys. Interestingly, C_{33} is much higher around 249 GPa, thus suggesting higher stiffness and stronger bonding along the c-axis. The anisotropy factors are utilized to assess a material's susceptibility to micro-cracks caused by thermal expansion. If anisotropy factor A = 1, the material is elastically isotropic in that shear plane. Our calculated A_1 and A_2 values of 1.843 and 1.344 for Ti_2VPt alloy in Figure 3 (b) deviate slightly from unity, which suggests that there is moderate anisotropy. This is true since $C_{33} > C_{11}$.

Figure 3 (c) shows a graph of the elastic moduli of Ti_2VPt alloys. The bulk modulus (B) evaluates the resistance of the material to compression, while G measures the resistance to distortion and E measures the material's stiffness. The Ti_2VPt alloy possesses higher bulk and Young's moduli values and lower shear moduli, which implies increased stiffness, mechanical hardness and resistance to deformation by external stresses.

To further investigate the ductility or brittleness of Ti_2VPt alloys in Figure 3 (d), Poisson's (ν) and Pugh's (k) ratios were computed. Poisson's ratio (ν) is a factor that measures the stability of a material against shear deformation [22]. A value higher or equal to 0.260 demonstrates ductility, or else brittle. The calculated ν is 0.321, which suggests ductility for Ti_2VPt alloys.

The Pugh ratio (k) [23] is used to predict the ductility or brittleness of solids. Accordingly, k is considered ductile if B/G > 1.75 and brittle if B/G < 1.75. From Figure 3(c), it was observed that the value of k is 2.460 greater than 1.75, suggesting ductility and thus the ability to withstand deformation against stress.

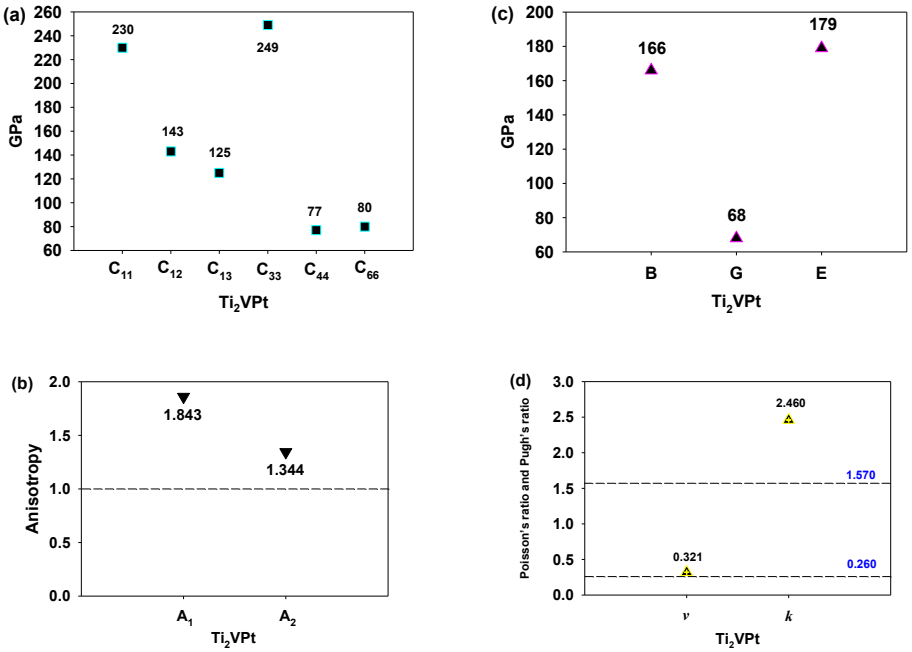

Fig. 3. The estimated graphs of (a) elastic constant (b) anisotropy (c) elastic moduli (d) Poisson's ratio (v) and. Pugh's ratio (k) of Ti_2VPt alloys.

The phonon dispersion frequencies along high symmetry lines across the Brillouin zone were computed to evaluate the dynamical stability of Ti_2VPt. If there are no negative frequencies/ soft modes along the high symmetry, the material is stable. In Figure 4, the Ti_2VPt alloy exhibited positive frequencies and no visible soft mode in the negative frequency, which is consistent with the calculated elastic constants in Figure 3(a). Therefore, the calculated phonon dispersion of the alloy indicates dynamical stability.

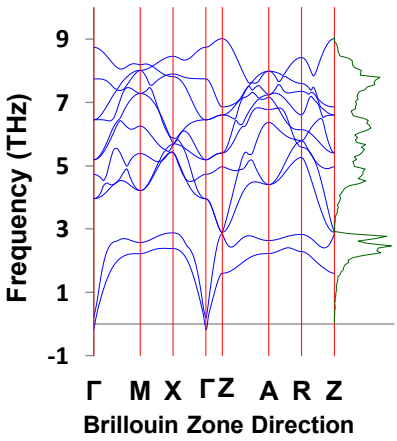

Fig. 4. The phonon dispersion curves for Ti_2PtV alloy.

4 Conclusion

Cluster expansion effectively determined the ground state structures and phase diagram of the Ti-Pt-V on the Pt sub-lattice, with the Ti_2VPt alloy identified as the most stable structure along the ground state line (-0.352 eV/atom). The mechanical characteristics of the Ti_2VPt alloy indicated that the system is mechanically stable. The phonon dispersion evaluation indicated vibrational stability in Ti_2PtV alloy. This study indicates that an incorporation of V stabilizes the TiPt shape memory alloys, rendering it a viable contender for higher-temperature applications.

The simulations were conducted using computer resources at the Materials Modelling Centre (MMC) at the University of Limpopo and the Centre for High Performance Computing (CHPC). The authors recognize. The authors recognise the South African Research Chair Initiative of the Department of Science and Innovation (DSI), the National Research Foundation, the Advanced Materials Initiative (AMI), and the University of Limpopo, all of which are acknowledged with deep gratitude.

Data availability statement: The data can be obtained on request from Mordecai Mashamaite. Email: mordecai.mashamaite@ul.ac.za

References

1. M.P. Mashamaite, H.R. Chauke, P.E. Ngoepe, The effects of Ru, Cu, Zr and Hf on mechanical properties in Ti-Pt high temperature shape memory alloys. IOP Conf. Ser.: Mater. Sci. Eng. **430**, 012019 (2018). https://doi.org/10.1088/1757-899X/655/1/012011
2. G.S. Firstov, J. Van Humbeeck, Y.N. Koval, High-temperature shape memory alloys: Some recent developments. Mater. Sci. Eng.: A **378**, 2–10 (2004). https://doi.org/10.1016/j.msea.2003.10.324
3. P. Kumar, U.V. Waghmare, First-principles phonon-based model and theory of martensitic phase transformation in NiTi shape memory alloy. Materialia (Oxf) **9**, 100602 (2020). https://doi.org/10.1016/j.mtla.2020.100602
4. J. Ma, I. Karaman, R.D. Noebe, High temperature shape memory alloys. Inter. Mater. Rev. **55**, 257–315 (2010). https://doi.org/10.1179/095066010X12646898728363
5. Y. Yamabe-Mitarai, TiPd- and TiPt-based high-temperature shape memory alloys: A review on recent advances. Metals **10**, 1531 (2020). https://doi.org/10.3390/met10111531
6. C. Declairieux, A. Denquin, P. Ochin, R. Portier, P. Vermaut, On the potential of $Ti_{50}Au_{50}$ compound as a high temperature shape memory alloy, Intermetallics **19**, 1461–1465 (2011). https://doi.org/10.1016/j.intermet.2011.05.028
7. T. Biggs, M.B. Cortie, M.J. Witcomb, L.A. Cornish, Martensitic transformations, microstructure, and mechanical workability of TiPt. Metall. Mater. Trans. A **32**, 1881–1886 (2001). https://doi.org/10.1007/s11661-001-0001-5
8. K. Otsuka, K. Oda, Y. Ueno, Min. Piao, T. Ueki, H. Horikawa, The shape memory effect in a $Ti_{50}Pd_{50}$ alloy. Scr. Metall. Mater. **29**, 1355–1358 (1993). https://doi.org/10.1016/0956-716X(93)90138-I
9. Y. Yamabe-Mitarai, T. Hara, S. Miura, H. Hosoda, Shape memory effect and pseudoelasticity of TiPt. Intermetallics **18**, 2275–2280 (2010). https://doi.org/10.1016/j.intermet.2010.07.011
10. R. Mahlangu, M.J. Phasha, H. R. Chauke, P. E. Ngoepe, Structural, elastic and electronic properties of equiatomic PtTi as potential high-temperature shape

memory alloy. Intermetallics **33**, 27–32 (2013). https://doi.org/10.1016/j.intermet.2012.09.021
11. A. Wadood, Y. Yamabe-Mitarai, TiPt–Co and TiPt–Ru high temperature shape memory alloys. Mater. Sci. Eng.: A **601**, 106–110 (2014). https://doi.org/10.1016/j.msea.2014.02.029
12. A. Wadood, M. Takahashi, S. Takahashi, H. Hosoda, Y. Yamabe-Mitarai, High-temperature mechanical and shape memory properties of TiPt–Zr and TiPt–Ru alloys. Mater. Sci. Eng.: A **564**, 34–41 (2013). https://doi.org/10.1016/j.msea.2012.11.069
13. P. Daswa, S. Chikosha, C.W. Siyasiya, Shape memory properties and transformation temperature of $Ti_{50-x}V_xPt_{50}$ alloy. Intermetallics **133**, 107154 (2021). https://doi.org/10.1016/j.intermet.2021.107154
14. S. Kadkhodaei, J.A. Muñoz, Cluster expansion of alloy theory: A review of historical development and modern innovations. JOM **73**, 3326–3346 (2021). https://doi.org/10.1007/s11837-021-04840-6
15. G. Kresse, J. Hafner, Ab initio molecular dynamics for liquid metals. Phys. Rev. B **47**, 558 (1993). https://doi.org/10.1103/PhysRevB.47.558
16. J. P. Perdew, K. Burke, M. Ernzerhof, Generalized gradient approximation made simple. Phys. Rev. Lett. 77, 3865–3868 (1996). https://doi.org/10.1103/PhysRevLett.77.3865
17. W. Setyawan, S. Curtarolo, High-throughput electronic band structure calculations: Challenges and tools. Comput, Mater. Sci. **49**, 299–312 (2010). https://doi.org/10.1016/j.commatsci.2010.05.010
18. G.W. Fernando, R. E. Watson, M. Weinert, Heats of formation of transition-metal alloys: Full-potential approach and the Pt-Ti system. Phys. Rev. B **45**, 8233–8238 (1992). https://doi.org/10.1103/PhysRevB.45.8233
19. G. Bozzolo, H.O. Mosca, R.D. Noebe, Phase structure and site preference behavior of ternary alloying additions to PdTi and PtTi shape-memory alloys. Intermetallics **15**, 901–911 (2007). https://doi.org/10.1016/j.intermet.2006.10.049
20. F. Mouhat, F. Coudert, Necessary and sufficient elastic stability conditions in various crystal systems. Phys. Rev. B **90**, (2014). https://doi.org/10.1103/PhysRevB.90.224104
21. R. Hill, The elastic behaviour of a crystalline aggregate. Proc. Phys. Soc. A **65**, 349 (1952). https://doi.org/10.1088/0370-1298/65/5/307
22. P. Ravindran, L. Fast, P. A. Korzhavyi, B. Johansson, J. Wills, O. Eriksson, Density functional theory for calculation of elastic properties of orthorhombic crystals: Application to $TiSi_2$, J. Appl. Phys. **84**, 4891–4904 (1998). https://doi.org/10.1063/1.368733
23. S.F. Pugh, XCII. Relations between the elastic moduli and the plastic properties of polycrystalline pure metals. Lond. Edinb. Dubl. Phil. Mag. **45**, 823–843 (1954). https://doi.org/10.1080/14786440808520496